

PULSED CO<sub>2</sub> LASER PROCESSING OF THIN ION-IMPLANTED SILICON LAYERS

R. B. James  
 Theoretical Division  
 Sandia National Laboratories  
 Livermore, California 94550

and

W. H. Christie  
 Analytical Chemistry Division  
 Oak Ridge National Laboratory  
 Oak Ridge, Tennessee 37831

Abstract

We show that extremely shallow ( $\leq 800 \text{ \AA}$ ) melt depths can be easily obtained by irradiating a thin heavily doped silicon layer with a CO<sub>2</sub> laser pulse. Since the absorption of the CO<sub>2</sub> laser pulse is dominated by free-carrier transitions, the beam heating occurs primarily in the thin degenerately doped film. For CO<sub>2</sub> pulse-energy densities exceeding a threshold value, surface melting occurs and the reflectivity of the incident laser pulse increases abruptly to about 90 %. This large increase in the reflectivity acts like a switch to reflect almost all of the energy in the remainder of the pulse, thereby greatly reducing the amount of energy available to drive the melt front to deeper depths in the material. Transmission electron microscopy shows no extended defects in the near-surface region after laser irradiation, and van der Pauw electrical measurements verify that 100% of the implanted arsenic dopant is electrically active.

Introduction

Pulsed laser processing of ion-implanted silicon has been applied extensively to the fabrication of high-efficiency solar cells.<sup>1</sup> It has been demonstrated that pulsed laser annealing is superior to thermal annealing for the removal of lattice damage caused by ion implantation, electrical activation of implanted dopants, and preservation of the minority carrier diffusion length in the base region of the solar cell.<sup>2</sup> Most of the advantages of laser annealing over conventional thermal processing result from the localization of thermal effects associated with the laser pulse and the increased control of several critical solar cell parameters (e.g., junction depth and free-carrier concentration).

There exists many reports on the use of pulsed lasers to melt ion-implanted silicon layers.<sup>3</sup> Almost all of these investigations have been conducted with a laser that has a photon energy greater than the bandgap, such as a ruby or excimer laser. Unfortunately, the energy deposited from a ruby or excimer laser always occurs within the absorbing layer at the surface, and one has little control over the penetration depth for a fixed photon energy. In order to melt extremely thin ( $\leq 800 \text{ \AA}$ ) layers with a ruby or excimer laser, one has to precisely control the pulse-energy density at a value close to the melt threshold, which is generally difficult due to beam reproducibility and spatial inhomogeneities. For low energy ( $< 10 \text{ keV}$ ) arsenic-implanted Si samples, we show in this paper that a pulsed CO<sub>2</sub> laser is particularly suitable for forming very shallow ( $< 800 \text{ \AA}$ ) melt depths by controlled heating of only the thin degenerately doped surface layer. After laser irradiation the resultant profile of electrically active arsenic shows a region near the surface having a concentration exceeding the equilibrium solid solubility limit and an intermediate region in which the density falls rapidly toward the n-p electrical junction, both of which are important to the manufacturing of n<sup>+</sup>pp<sup>+</sup> solar cells with high conversion efficiencies.

For CO<sub>2</sub> laser radiation ( $\lambda = 10 \mu\text{m}$ ), the absorption of the pulse energy in a shallow arsenic implanted Si layer is dominated by free-electron transitions within the conduction band. Since the free-electron concentration in the thin surface film can be several orders of magnitude greater than the underlying substrate, one can preferentially deposit the energy of the laser pulse in the thin film at the surface. If the duration of the pulse is short compared to the time required to conduct the heat out of the shallow surface layer, then the CO<sub>2</sub>-laser-induced heating occurs only in the thin arsenic-implanted layer where the free-carrier density is large. Because molten silicon is metallic, the onset of surface melting causes the reflectivity of the sample to increase abruptly to about 90 %, which is much larger than the reflectivity increase of a ruby or excimer laser pulse. This large increase of the reflectivity upon melting acts like a switch to reject most of the energy in the remainder of the CO<sub>2</sub> laser pulse, thereby reducing the amount of energy available to further heat the surface and drive the melt front to considerably deeper depths in the material. Furthermore, for applications where one has both heavily doped and undoped areas in the near-surface region, one can spatially select the heavily doped regions for beam heating, without causing significant heating of the adjacent undoped material.<sup>4-5</sup> Thus, one can use a relatively large CO<sub>2</sub> laser pulse to simultaneously process many ion-implanted regions on the same or on different silicon wafers.

Experimental

A gain-switched, TEA CO<sub>2</sub> laser was used to generate the pulses at a wavelength of 10.6  $\mu\text{m}$ . The laser

Accepted for publication at the proceeding of the  
 11th Internat Conf on Lasers and Laser Applications,  
 1989  
 Dec 5-9, Lake Tahoe, NV

MASTER

DISTRIBUTION OF THIS DOCUMENT IS UNLIMITED

was operated with low nitrogen content in the gas mix, so that the amplitude of the long tail on the pulses could be greatly suppressed. About 80% of the energy in each pulse was contained in the form of a nearly Gaussian peak of 60-ns duration (FWHM). The remaining 20% of the pulse energy was in a second pulse that was delayed by about 300 ns from the first pulse and had a duration of 250 ns (FWHM). For the energy densities considered in this report, the second pulse makes a negligible contribution to the melt depths and durations of surface melting. As a result, the pulse-energy densities quoted in this paper are for the energy in the 60-ns primary pulse only.

The output pulse was diverged by a spherical convex mirror with a 1-m radius of curvature. The diverging beam was later collimated by a spherical concave mirror with 2-m radius of curvature. The collimated beam then impinged on a CO<sub>2</sub> laser beam integrator which spatially homogenized the beam to within  $\pm 10\%$ . The dimensions of the laser pulses were 12x12 mm in the target plane of the integrator. The energy density at the sample surface was adjusted by using additional lenses to change the spot size and linear attenuators to change the total energy in each pulse. A photon-drag detector and volume absorbing calorimeter were used to measure the intensity and energy of the laser pulses, respectively.

The samples used in the experiment were 340- $\mu\text{m}$  thick, boron-doped silicon (100) wafers which, prior to implantation, had an electrical resistivity of  $2\text{-}3\text{ }\Omega\text{-cm}$  at room temperature. This resistivity corresponds to a free-hole concentration of approximately  $6 \times 10^{15} \text{ cm}^{-3}$  and hole mobility of about  $350 \text{ cm}^2/\text{V}\cdot\text{s}$ . The samples were implanted on one side with As<sup>+</sup> ions at an energy of 5 keV to a dose of  $2 \times 10^{15} \text{ cm}^{-2}$ , resulting in an arsenic profile that is peaked at about 70  $\text{\AA}$  from the surface with a standard deviation of about 25  $\text{\AA}$ . The samples were next thermally annealed at 873 K for twelve minutes to increase the fraction of electrically active arsenic and thereby increase the coupling of the CO<sub>2</sub> laser radiation to the near-surface region.<sup>6</sup> The concentration of arsenic near the peak of the implanted profile exceeds the solid solubility limit, resulting in the formation of arsenic-rich precipitates in part of the implanted layer. Van der Pauw measurements on the thermally annealed samples showed a carrier density of  $6.2 \times 10^{14} \text{ cm}^{-3}$ , carrier mobility of  $30 \text{ cm}^2/\text{V}\cdot\text{s}$ , and sheet resistivity of 335  $\Omega/\text{sq}$ .

The free-electron concentration in the first 200  $\text{\AA}$  is greater than  $10^{20} \text{ cm}^{-3}$ , so that the absorption coefficient ( $\alpha$ ) of the CO<sub>2</sub> laser radiation is large ( $> 2 \times 10^4 \text{ cm}^{-1}$ ) near the surface. The lightly doped substrate is relatively transparent to 10.6- $\mu\text{m}$  radiation and has a value of less than  $10 \text{ cm}^{-1}$  at room temperature. Thus, the pulse-energy deposition is primarily in the thin film at the surface.

The samples were irradiated in air by CO<sub>2</sub> laser pulses at different energy densities. Van der Pauw measurements were used to determine the changes in the carrier concentration, carrier mobility, and sheet resistivity. A Fourier transform infrared spectrometer was utilized to study the laser-induced modifications in the optical properties of the near-surface region. The microstructure of the near-surface region was investigated by cross-section transmission electron microscopy. Secondary ion mass spectrometry was utilized to measure the redistribution of the implanted arsenic and to investigate the possibility of controlling the dopant profiles by varying the energy density of the laser pulses.

### Results and Discussion

Van der Pauw measurements were performed on the laser-irradiated samples, and the results showed that for pulse-energy densities ( $E_L$ ) greater than about  $5 \text{ J/cm}^2$ , significant changes in the electrical properties of the ion-implanted layer occurred (see Table I). For values of  $E_L$  between 5.0 and 7.5  $\text{J/cm}^2$ , there was an increase in the electron concentration ( $N_s$ ) and a decrease in the sheet resistivity ( $\rho$ ) with increasing  $E_L$ . The increase in  $N_s$  results from the partial melting of the arsenic-implanted layer and subsequent electrical activation of the arsenic upon solidification of the molten layer. At pulse-energy densities greater than about  $7.5 \text{ J/cm}^2$ , the melt front penetrated to a depth exceeding the implantation-damaged surface layer, and 100%-activation of the implanted arsenic was observed. At these higher values of  $E_L$ , the implanted arsenic redistributes to deeper depths, and the electron mobility begins to increase monotonically with  $E_L$  due to the reduced rate of carrier scattering by the ionized arsenic dopants.

The CO<sub>2</sub>-laser-induced melting of the near-surface region also causes significant changes in the infrared optical properties of the silicon samples. A Fourier transform infrared spectrometer was used to obtain

Table I. Electrical properties of the arsenic-implanted silicon samples as a function of the incident pulse-energy density. Here,  $E_L$  is the energy density,  $N_s$  is the electron concentration,  $\rho$  is the sheet resistivity, and  $\mu$  is the carrier mobility.

$E_L (\text{J/cm}^2)$	$N_s (10^{15} \text{ cm}^{-2})$	$\rho (\Omega/\text{sq})$	$\mu (\text{cm}^2/\text{V}\cdot\text{s})$
0.0	0.62	335	30
4.4	0.65	318	30
5.3	0.96	233	28
6.1	1.62	135	29
6.8	1.81	104	33
7.5	2.00	92	34
8.4	2.01	76	41
9.2	2.00	51	59
9.9	1.99	48	65

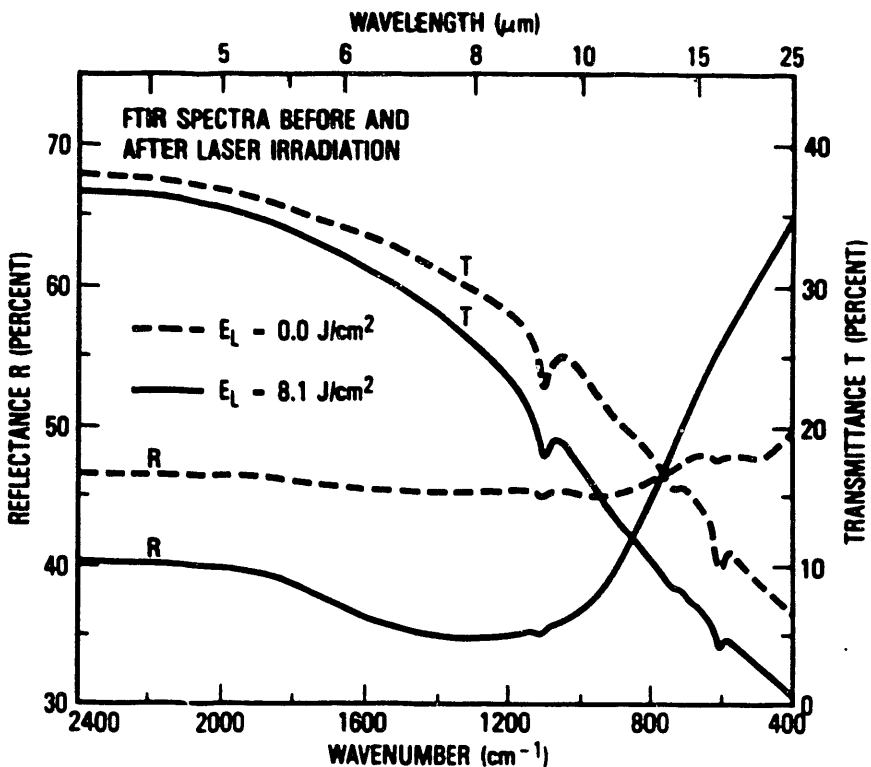


Fig. 1 Reflectance and transmittance spectra for an unirradiated sample and a sample after irradiation at  $E_L = 8.1 \text{ J/cm}^2$ .

transmittance and reflectance spectra before and after laser irradiation. Figure 1 shows the total reflectance and transmittance spectra in the 400 to  $2400 \text{ cm}^{-1}$  range for an unirradiated sample and a sample irradiated at  $E_L = 8.1 \text{ J/cm}^2$ . After irradiation at  $E_L = 8.1 \text{ J/cm}^2$ , the total reflectance was found to change from 45 % to 38 %, and the total transmittance changed from 22 % to 14 % for light having a wavelength of  $10.6 \mu\text{m}$ . The increase in the free-carrier absorption is consistent with the measured increase ( $\sim 223 \text{ \%}$ ) in the electron concentration of the arsenic-implanted layer (see Table I).

We used cross-section transmission electron microscopy (TEM) to investigate the presence of extended defects in the ion-implantation-damaged layer. Figure 2(a) is a micrograph of a specimen that has been irradiated by a pulse having an energy density of  $8.1 \text{ J/cm}^2$ . At this pulse-energy density, the surface layer contained no extended defects with a size larger than  $20 \text{ \AA}$ , which is the smallest size that can be clearly resolved in the micrograph. In addition, the van der Pauw measurements on the sample showed that all of the implanted arsenic was electrically active. The TEM micrograph, together with the electrical measurements, indicates that the entire implantation-damaged layer was melted by the laser pulse and that liquid-phase epitaxial regrowth of the molten layer occurred.

Another sample was also irradiated at  $8.1 \text{ J/cm}^2$  and then heated in a furnace to  $973 \text{ K}$  for ten minutes to study the precipitation of the implanted arsenic. Fig. 2(b) shows a cross-section TEM micrograph of the specimen after furnace treatment. Arsenic-rich precipitates are observed to depths of about  $250 \text{ \AA}$  throughout the near-surface region.

Secondary ion mass spectrometry (SIMS) was used to measure the arsenic profiles before and after laser irradiation. The results are shown in Fig. 3 for several different energy densities. For  $E_L$  less than  $5 \text{ J/cm}^2$ , no redistribution of the implanted arsenic was observed. For higher pulse-energy densities, the arsenic was found to diffuse to deeper depths due to the penetration of the melt front and subsequent liquid-phase diffusion in the near-surface region. The amount of redistribution was relatively small for pulse-energy densities in the range of 5 to  $8 \text{ J/cm}^2$ . For  $E_L > 8 \text{ J/cm}^2$ , the maximum depth of As diffusion begins to increase much more rapidly with increasing  $E_L$  and reaches depths of over  $1000 \text{ \AA}$  for pulse-energy densities greater than  $10 \text{ J/cm}^2$ . No surface segregation behavior was observed in any of the laser irradiated arsenic-implanted specimens.

#### Conclusions

We have shown that extremely shallow melt depths can be easily obtained by  $\text{CO}_2$  laser annealing of low-



Fig. 2 The top photograph shows a cross-section TEM micrograph of a sample after irradiation by a  $\text{CO}_2$  laser pulse having an energy density of  $8.1 \text{ J/cm}^2$ . The bottom photograph shows a different sample that was heated in a furnace at 973 K for ten minutes after being irradiated by a laser pulse at  $E_L = 8.1 \text{ J/cm}^2$ . The location of the surface is shown by an arrow in each photo.

energy ( $\leq 5 \text{ keV}$ ) arsenic-implanted silicon layers. Similar results are expected for other silicon samples having a thin degenerately doped surface layer and an underlying lightly doped substrate. The primary advantages of using a  $\text{CO}_2$  laser to achieve very shallow melt depths, as compared to a ruby or excimer laser, are that the pulse energy is deposited only in the thin heavily doped layer at the surface and the  $\text{CO}_2$ -laser-induced melting of the surface layer causes the reflectivity to jump abruptly to a value of about 90 %. The large and sudden increase in the reflectivity upon melting acts like a switch to reflect most of the energy in the remainder of the laser pulse and thereby greatly reduce the amount of pulse energy available for driving the melt front to deeper depths. For a 60-ns pulse and pulse-energy densities ( $E_L$ ) greater than about  $7 \text{ J/cm}^2$ , we find that all of the ion implanted arsenic is electrically active and the near-surface region is free of any extended defects.

#### Acknowledgments

We would like to thank R. P. Wood, J. Narayan, G. A. Geist, D. H. Lovndes, P. H. Fleming, H. L. Burcham, Jr., D. C. Lind, A. J. Antolak, K. F. McCarty, and M. I. Baskes for many useful discussions. We would also like to acknowledge support from the U. S. Department of Energy.

#### References

1. See, for example, R. T. Young, G. A. van der Leeden, R. L. Sandstrom, R. P. Wood and R. D. Westbrook, *Appl. Phys. Lett.* 43, 666 (1983).
2. R. T. Young and R. P. Wood, *Ann. Rev. Mater. Sci.* 12, 323 (1982).
3. See, for example, *Pulsed Laser Processing of Semiconductors*, Vol. 23, edited by R. P. Wood, C. V. White and R. T. Young (Academic, New York, 1984).
4. R. B. James, G. A. Geist, R. T. Young, W. H. Christie and F. A. Greulich, *J. Appl. Phys.* 62, 2981 (1987).
5. R. B. James, J. Narayan, R. P. Wood, D. K. Ottesen and K. F. Siegfriedt, *J. Appl. Phys.* 57, 4727 (1985).
6. F. A. Trumbore, *Bell Syst. Tech. J.* 39, 205 (1960).
7. W. G. Spitzer and H. Y. Fan, *Phys. Rev.* 106, 882 (1957).
8. W. G. Spitzer and H. Y. Fan, *Phys. Rev.* 108, 268 (1957).

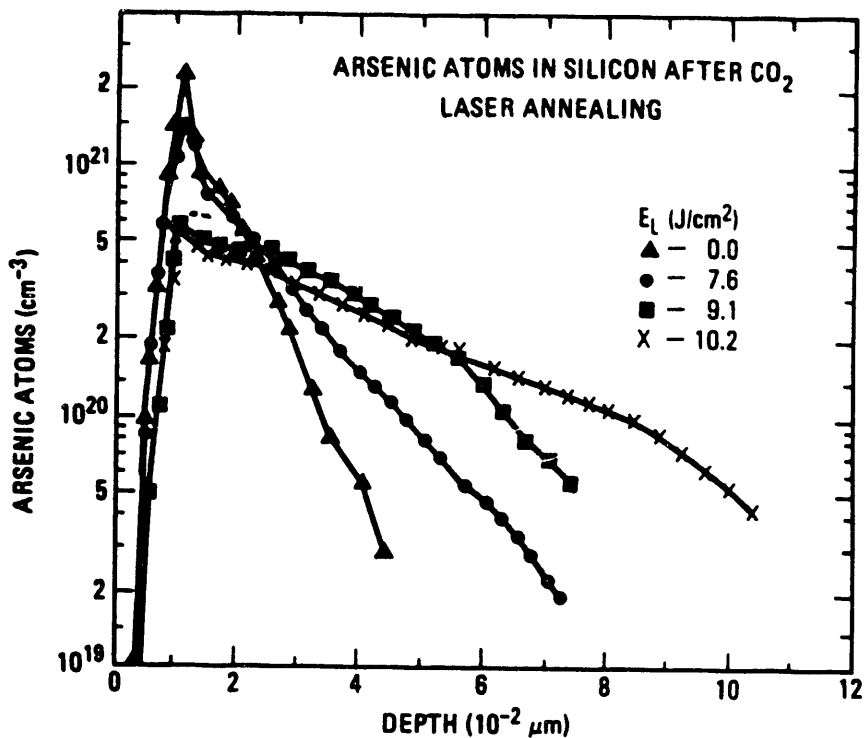


Fig. 3 SIMS measurements of arsenic atoms as a function of depth for samples irradiated at different energy densities. The four curves show the arsenic profiles for the following samples:  $\blacktriangle$ , an unirradiated sample;  $\bullet$ , a sample irradiated at  $E_L = 7.6 \text{ J/cm}^2$ ;  $\blacksquare$ , a sample irradiated at  $E_L = 9.1 \text{ J/cm}^2$ ; and  $\times$ , a sample irradiated at  $E_L = 10.2 \text{ J/cm}^2$ .

## DISCLAIMER

This report was prepared as an account of work sponsored by an agency of the United States Government. Neither the United States Government nor any agency thereof, nor any of their employees, makes any warranty, express or implied, or assumes any legal liability or responsibility for the accuracy, completeness, or usefulness of any information, apparatus, product, or process disclosed, or represents that its use would not infringe privately owned rights. Reference herein to any specific commercial product, process, or service by trade name, trademark, manufacturer, or otherwise does not necessarily constitute or imply its endorsement, recommendation, or favoring by the United States Government or any agency thereof. The views and opinions of authors expressed herein do not necessarily state or reflect those of the United States Government or any agency thereof.

END

DATE  
FILMED

12/03/91

